

Vibration Suppression Control Using an Equivalent Rigid-Body Observer

Yasufumi Yoshiura* Member, Shouta Kawahara* Member
Daichi Horimai* Non-member, Tetsuya Asai* Member
Yasuhiko Kaku* Senior Member

(Manuscript received June 1, 2017, revised Feb. 26, 2018)

In a mechanical system whose control target is known, a precise control model of the controlled object is defined using a system identification method, and an optimum control method is selected and designed using modern control theory. However, with a general-purpose servo drive, the controlled model cannot be defined completely in advance. This paper proposes a method of suppressing mechanical resonance with an equivalent rigid body observer based on a motor model, which can be installed without clarifying the controlled object model. In addition, the applicability of the proposed method to both semi-closed and full-closed controlled systems is confirmed through experiments.

Keywords: vibration suppression control, equivalent rigid-body velocity

1. Introduction

In machines using generally sold servo motors, there is increasing demand for operating machines at high speed and in high precision to improve throughput and process accuracy, reduce vibration during conveyance, and so on. In order to operate stably at high speed, it is desired to set the feedback gain as high as possible, but since the vibration of the control system is caused by the mechanical resonance characteristics and the calculation time of the control system, the feedback gain is restricted.

In case of a general-purpose servo drive system sold in combination with a servo amplifier and a servomotor, the only known controlled model by the manufacturer is the motor. Therefore the controlled model of mechanical system can not be defined in advance. In addition, it is necessary to combine with external sensors such as linear scales.

Furthermore, a general-purpose servo amplifier has already implemented the control method by manufacturer, and the user has to accomplish the gain setting. However, users who are unfamiliar with control technique may have difficulties in tuning the gain, so it is required that implemented control method is applicable to wide range control objects, and the control method to be applied and the tuning procedure of the gain are clear.

In this respect, the implemented control algorithm in a general-purpose servo amplifier has a traditionally modeled motor and a rigid load as a controlled object, and a dual feedback loop which position signal feedback loop is provided outside the feedback loop of the motor velocity. In case of semi-closed control, the velocity signal and the position signal are fed back from the encoder attached to the motor. On the other hand, in the full-closed control, there is a case where the velocity signal and the position signal are fed back from

an external sensor such as a linear scale or the position signal, and the velocity signal is fed back from the encoder attached to the motor. The latter one is semi-closed control for velocity feedback. A control algorithm to be incorporated in a general-purpose servo amplifier is required to be able to cope with either case.

Concerning control system instability caused by mechanical resonance, if the vibration frequency is sufficiently higher than the frequency band of the velocity feedback loop against the control system, vibration can be reduced by tuning the parameters of the implemented notch filter and low pass filter. However, when the filter mentioned above is applied when the vibration frequency is close to the cutoff frequency of the velocity feedback loop, the control loop tends to become unstable, and in many cases, the control gain has to be reduced.

To solve the instability of control system due to control calculation time, a method of compensation for delay⁽⁵⁾ and a gain setting method considering delay in calculation time⁽⁶⁾ are proposed. In case of performing the delay compensation, the gain in the high frequency band increases due to the frequency characteristic, then mechanical resonance may be induced. In the gain setting method considering the delay, although it is possible to select the allowable upper limit of the gain, the delay can not be reduced, so it is difficult to set the high gain in the end.

From the above, stabilization of mechanical resonance characteristics is an essential task for high-speed and high-precision mechanical operation.

In case of full-closed control, a method of stabilizing by feeding back the difference velocity between the encoder attached to the motor and the external sensor is also effective. But an encoder is required on the motor side. However, this method can not be applied to the linear motor because only the external sensor is attached.

As examples of stabilizing the mechanical resonance characteristics, a method of inputting the same signal to the reference model and the real system, aiming for a response similar

* YASKAWA ELECTRIC CORPORATION
480 Kamifujisawa, Iruma, Saitama 358-8555, Japan

to the model by processing the output difference between them and returning them to the input⁽¹¹⁾ or feed-backing the estimated state quantity using the observer are used⁽⁵⁾⁻⁽¹⁰⁾. In the former case, the parameter fluctuation has an adverse effect. For example, when the moment of inertia changes, removal of the low frequency signal becomes insufficient, and it is impossible to extract only the mechanical resonance signal. Also, in case of a model with an ideal state in which there is no disturbance or the like, the disturbance signal components such as the frictional force of the transmission mechanism and the reaction force from the load can not be removed. In the latter case, in many cases, it is necessary to define the spring constant and the damping coefficient as the nominal model of the observer in order to estimate the state quantity. Although a method of using a rigid body observer⁽¹²⁾ has been proposed, the observer is a substitute for a differentiator and is not intended to extract vibration components.

In a system whose control target is known, a detailed control model of the control target is defined using a system identification method⁽¹⁾⁻⁽⁴⁾ and an optimum control method can be selected/designed. However dedicated equipment and skilled engineers are necessary. For this reason, it is difficult for ordinary engineers to define the parameters necessary for the observer in the scene of tuning a general-purpose servo amplifier at the machine builder. General-purpose servo amplifier have to stabilize the mechanical resonance characteristics with almost the same effort as servo gain tuning at the manufacturing site. This paper explains the vibration control method with the equivalent rigid body observer based on the motor and the rigid body load as an example of a control algorithm that can be implemented even if the characteristics of the controlled object is unknown. In addition, we report the experimental results which applies vibration suppression control to the semi-closed control system and full-closed control system of 2 inertia resonance system.

2. Modeling of Mechanical System

Consider a 2 inertia system as a controlled object which has a single vibration frequency. 2 inertia resonant system can be described as the following equation.

$$J_M \ddot{\theta}_M + K(\theta_M - \theta_L) = T_M \quad \dots\dots\dots (1a)$$

$$J_L \ddot{\theta}_L + K(\theta_L - \theta_M) = 0 \quad \dots\dots\dots (1b)$$

Where

T_M : Motor torque

θ_M : Motor rotation angle

θ_L : Load rotation angle

K : Spring constant

J_M : Rotor moment of inertia

J_L : Load moment of inertia

For simplicity, the viscous damping term is set to 0. The transfer function from the motor torque to the motor velocity and the transfer function from the motor torque to the load velocity are as follows.

$$G_M(s) = \left(\frac{1}{J_M + J_L} \cdot \frac{1}{s} \right) \cdot \left(\frac{s^2 + \omega_a^2}{\omega_a^2} \cdot \frac{\omega_r^2}{s^2 + \omega_r^2} \right) \quad \dots\dots (2a)$$

$$G_L(s) = \left(\frac{1}{J_M + J_L} \cdot \frac{1}{s} \right) \cdot \left(\frac{\omega_r^2}{s^2 + \omega_r^2} \right) \quad \dots\dots\dots (2b)$$

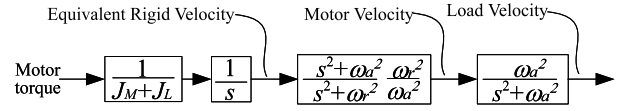


Fig. 1. Block diagram

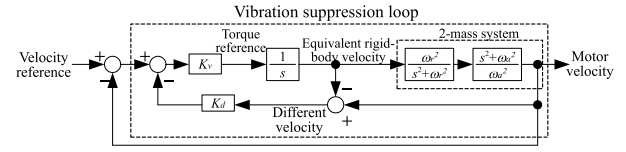


Fig. 2. Control block diagram of velocity P control including 2 inertia system (Semi-closed control system)

ω_r , ω_a of Eq. (2) are as follows.

$$\omega_r = 2\pi f_r = \sqrt{K \left(\frac{1}{J_M} + \frac{1}{J_L} \right)} \quad \dots\dots\dots (3a)$$

$$\omega_a = 2\pi f_a = \sqrt{\frac{K}{J_L}} \quad \dots\dots\dots (3b)$$

The frequency characteristic on the motor is a second order resonance characteristic having a dip of antiresonance frequency f_a defined by Eq. (2a) and a peak of resonance frequency f_r .

It can be seen that only the peak of the resonance frequency f_r is generated on the load side (Eq. (2b)). In Eq. (2), the first term ($1/s$ term) common in the motor side and the load side means a rigid body system, so we call this “equivalent rigid body” in this paper.

Equation (2a) and Eq. (2b) are represented in the block diagram collectively in Fig. 1. Note that the equivalent rigid body velocity differs from the motor velocity in Fig. 1.

3. The Elements of Vibration Suppression Control

In Eq. (2a) and Eq. (2b), the transfer functions differ between the motor side and the load side, but if the common term is used, vibration suppression control becomes possible. The conventional method attenuates the vibration caused by mechanical resonance by feeding back the difference between the load velocity including the motor velocity and the resonance characteristic⁽⁸⁾⁽⁹⁾. However, vibration suppression effect can be obtained by using equivalent rigid body velocity and motor velocity without using load velocity.

3.1 Principle of Vibration Suppression Control of Semi-closed System First, consider velocity P control including 2 inertia system as shown in Fig. 2. In Fig. 2, the total moment of inertia is set to “1” for simplicity, and assume that the converted velocity value from the encoder, which is attached to the motor, is fed back to the semi-closed control.

The transfer function of the open loop from the velocity error input to the vibration suppression unit output (output multiplied by the velocity difference by K_d) is as follows.

$$\begin{aligned} G_{open}(s) &= \frac{K_d K_v}{s} \left(\frac{s^2 + \omega_a^2}{s^2 + \omega_r^2} \cdot \frac{\omega_r^2}{\omega_a^2} - 1 \right) \\ &= \frac{K_d K_v}{s} \left(\frac{\omega_r^2}{\omega_a^2} - 1 \right) \frac{s^2}{s^2 + \omega_r^2} \end{aligned}$$

$$= K_d K_v \left(\frac{\omega_r^2}{\omega_a^2} - 1 \right) \frac{s}{\omega_r^2} \frac{\omega_r^2}{s^2 + \omega_r^2} \dots \dots \dots (4)$$

Equation (4) shows that it includes mechanical resonance characteristics (Eq. (2)). Therefore, the vibration waveform of the mechanical resonance characteristic can be observed in the output of the vibration suppression control section. Normally, since the resonance frequency ω_r is higher than the anti-resonance frequency ω_a , the following inequality holds in Eq. (4).

$$\frac{\omega_r^2}{\omega_a^2} - 1 > 0 \dots \dots \dots (5)$$

Therefore, the closed-loop transfer function from the velocity error to the motor velocity is given as follows.

$$\begin{aligned} G_{close}(s) &= \frac{1}{1 + G_{open}} \cdot \frac{K_v}{s} \frac{\omega_r^2}{s^2 + \omega_r^2} \frac{s^2 + \omega_a^2}{\omega_a^2} \\ &= \frac{1}{1 + K_d K_v \left(\frac{\omega_r^2}{\omega_a^2} - 1 \right) \frac{s}{s^2 + \omega_r^2}} \cdot \frac{K_v}{s} \frac{\omega_r^2}{s^2 + \omega_r^2} \frac{s^2 + \omega_a^2}{\omega_a^2} \\ &= \frac{s^2 + \omega_r^2}{s^2 + \omega_r^2 + K_d K_v \left(\frac{\omega_r^2}{\omega_a^2} - 1 \right) s} \cdot \frac{K_v}{s} \frac{s^2 + \omega_a^2}{s^2 + \omega_r^2} \frac{\omega_r^2}{\omega_a^2} \\ &= \frac{K_v}{s} \frac{\omega_r^2}{s^2 + K_d K_v \left(\frac{\omega_r^2}{\omega_a^2} - 1 \right) s + \omega_r^2} \cdot \frac{s^2 + \omega_a^2}{\omega_a^2} \dots \dots \dots (6) \end{aligned}$$

Equation (6) can be regarded as a form in which attenuation is added to the resonance side of the 2 inertia resonance system.

3.2 Principle of Vibration Suppression Control of Full-closed System Next, consider the case of full-closed control in which the converted velocity value from the position signal of the sensor, attached at the tip of the load, to be fed back. Since the anti-resonance term disappears as shown in Eq. (2b), the control block diagram of Fig. 2 becomes as shown in Fig. 3. The transfer function of the open loop from the velocity error to the output of the vibration suppression unit (the output multiplying the velocity difference by K_d) is as follows.

$$\begin{aligned} G_{open}(s) &= \frac{K_d K_v}{s} \left(\frac{\omega_r^2}{s^2 + \omega_r^2} - 1 \right) \\ &= \frac{K_d K_v}{s} \frac{-s^2}{s^2 + \omega_r^2} \\ &= \frac{-K_d K_v s}{\omega_r^2} \frac{\omega_r^2}{s^2 + \omega_r^2} \dots \dots \dots (7) \end{aligned}$$

Equation (7) shows that it includes mechanical resonance characteristics (Eq. (2)) as well as semi-closed control.

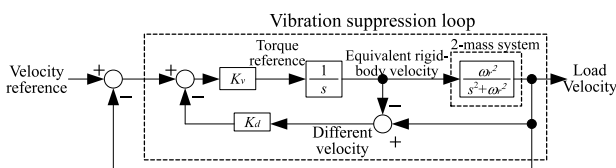


Fig. 3. Control block diagram of velocity P control including 2 inertia system (Full-closed control system)

Therefore, the vibration waveform can be observed in the output of the vibration suppression control loop. The closed-loop transfer function from the velocity error to the motor velocity is given as follows.

$$\begin{aligned} G_{close}(s) &= \frac{1}{1 + G_{open}} \cdot \frac{K_v}{s} \frac{\omega_r^2}{s^2 + \omega_r^2} \\ &= \frac{1}{1 - \frac{K_d K_v s}{s^2 + \omega_r^2}} \cdot \frac{K_v}{s} \frac{\omega_r^2}{s^2 + \omega_r^2} \\ &= \frac{s^2 + \omega_r^2}{s^2 + \omega_r^2 - K_d K_v s} \cdot \frac{K_v}{s} \frac{\omega_r^2}{s^2 + \omega_r^2} \\ &= \frac{K_v}{s} \cdot \frac{\omega_r^2}{s^2 - K_d K_v s + \omega_r^2} \dots \dots \dots (8) \end{aligned}$$

From Eq. (8), it can be seen that attenuation can be added to the resonance of 2 inertia system by setting the sign of K_d to be negative in case of full-closed control also.

4. The Realization of the Proposed Method

The previous chapter shows that if equivalent rigid body velocity can be detected, mechanical resonance characteristics can be attenuated in semi-closed control and full-closed control. However, since the equivalent rigid body velocity can not be detected in reality, it is estimated from the detectable motor velocity by using the observer.

4.1 First Order Observer Design With a given a state variable vector $x(t)$, one-dimensional control input $u(t)$, and one-dimensional observation output $y(t)$, the controlled object can be expressed as the following state equation.

$$\dot{x}(t) = Ax(t) + bu(t) \dots \dots \dots (9a)$$

$$y(t) = cx(t) \dots \dots \dots (9b)$$

Since the motor system can be approximated by an integrator that generates velocity by integrating torque, the coefficients of Eq. (9) can be expressed as Eq. (10) as an equivalent rigid body concretely.

$$A = 0, b = 1, c = 1 \dots \dots \dots (10)$$

In the Eq. (9), since (c, A) are observable, the identical observer of Eq. (11a) can be constructed. Moreover, the estimated value $\hat{y}(t)$ of the equivalent rigid body velocity can be obtained from the state estimate value in Eq. (11b).

$$\dot{\hat{x}}(t) = (A - kc)\hat{x} + ky(t) + bu(t) \dots \dots \dots (11a)$$

$$\hat{y}(t) = c\hat{x}(t) \dots \dots \dots (11b)$$

Where $\hat{x}(t)$ is the estimated value of state $x(t)$ and k is the gain vector of the observer. Since the torque command value has to input to $u(t)$ of Eq. (11a) and because it is identity observer so the true value of equivalent rigid body velocity should be used in $y(t)$, however it is approximated by motor velocity $y_m(t)$ which includes vibration. Furthermore, the observer gain k is selected so that the observer can not respond to the vibration component, which improves the approximation accuracy. In Fig. 4(a), since the difference between the motor velocity $y_m(t)$ and the estimated equivalent rigid body velocity is the vibration component, the vibration component can be estimated by Eq. (12).

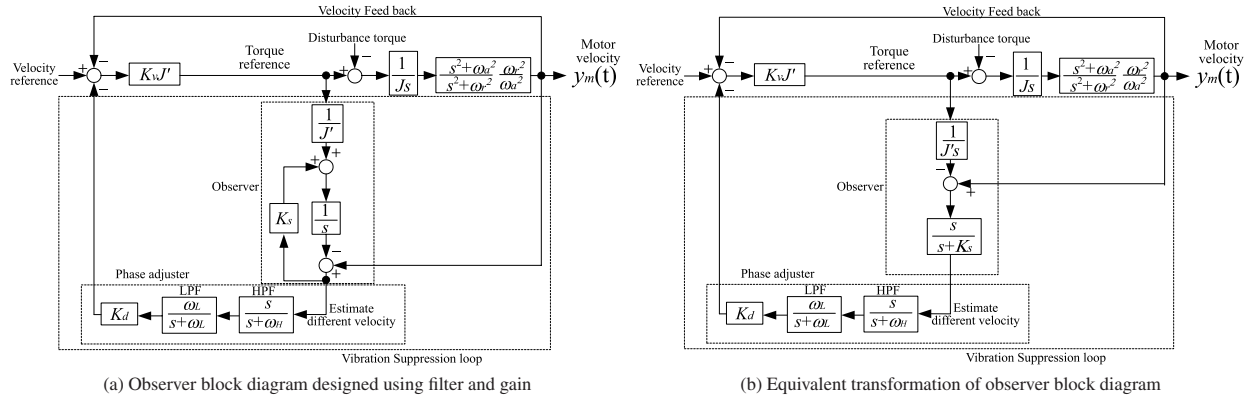


Fig. 4. Vibration compensate method with equivalent Rigid-Body Observer

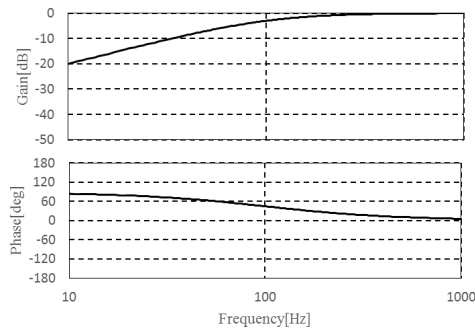


Fig. 5. Observer frequency characteristics

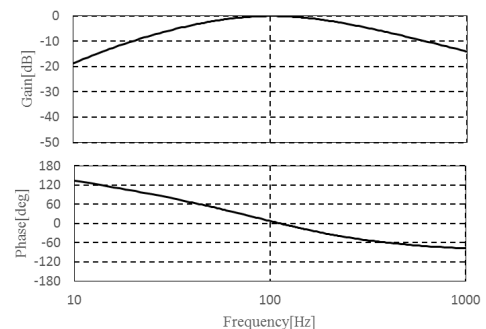


Fig. 6. Frequency characteristics of observer, phase compensator and high-pass filter

$$\hat{r}(t) = y_m(t) - \hat{y}(t) = y_m(t) - \mathbf{c}\hat{\mathbf{x}}(t) \dots \dots \dots (12)$$

Figure 4(b) shows the block diagram whose inside of the observer is modified, and the difference signal of the estimated value of the equivalent rigid body velocity and the motor velocity is indicated. The difference signal is generated from the observer through a block equivalent to the high pass filter. This is the same principle of vibration suppression control shown in Section 3.1. The frequency characteristic from the difference between the motor velocity $y_m(t)$ and the estimated equivalent rigid body velocity to the observer output is as shown in Fig. 5 where the observer gain is set to 100 Hz as an example.

4.2 Design of Phase Adjuster As shown in Fig. 5 in the previous section, since the estimated vibration phase advances depending on the relationship between the observer gain and the vibration frequency, it is necessary to eliminate the phase shift. As the simplest phase adjuster, a 1st order low pass filter is added in series at the observer output. Up to this point, although the influence of friction is not considered as a controlled object, usually friction can not be ignored in an actual mechanical system. Although the observer in Fig. 4(b) has the first-order high-pass characteristic, the steady disturbance can not be excluded because it is connected to the high-pass characteristic through the integral element from the disturbance. Therefore, in order to eliminate steady disturbance, a 1st order high pass filter is added in series at the observer output. Since the amplitude of the vibration frequency, which to be estimated, decreases by adding the low pass filter, restore the amplitude by adding the gain in series. Figure 6 shows the frequency characteristics of the difference between the estimated equivalent rigid body

velocity and the motor velocity $y_m(t)$ and the gain multiplied. At this time, the observer gain is 628.3/s, the cutoff frequency of the low-pass filter is 100 Hz, and the cutoff frequency of the high-pass filter is 15 Hz. From Fig. 6, assuming that the vibration frequency to be estimated is 100 Hz, close enough phase and amplitude can be estimated. In other words, the velocity difference in Fig. 1 and Fig. 2 in the previous section can be realized with observer, low pass filter, high pass filter and gain as shown in Fig. 4(a).

5. Experimental Results

Experiments were conducted using the equipment shown in Fig. 7. In this device, an external encoder for control was attached to the inertial load. The inertial load was connected to the servomotor with an elastic coupling. This external encoder was used to build a full-closed system. Similarly, an encoder was attached to the servo motor to build a current control and semi-closed system.

A dedicated motor driver was used for motor control with current/velocity control. We installed the proposed method in the motor driver and performed experiment.

Figure 8 shows frequency characteristics from motor torque to motor velocity (semi-closed system) and motor torque to external encoder velocity (full-closed system) of the experimental equipment. Focusing on the frequency characteristics of the semi-closed system, the anti-resonance frequency is 198 Hz and the resonance frequency is 662 Hz. The frequency characteristic of the full-closed system is only with the resonance frequency, 662 Hz.

5.1 Vibration Suppression Effect of Semi-closed System In the semi-closed system, the velocity loop is

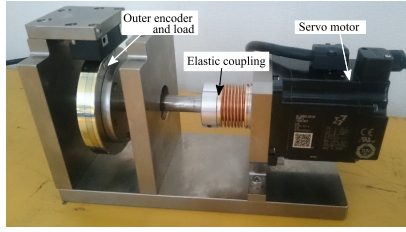


Fig. 7. Appearance of experimental equipment

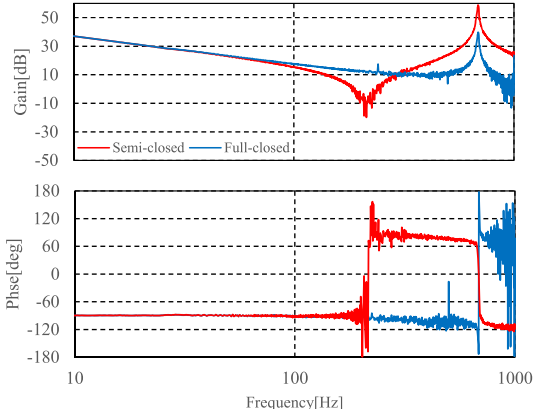


Fig. 8. Frequency characteristics of experimental equipment

Table 1. Control gain

	Semi-closed	Full-closed
Velocity loop proportional gain	188.5/s	754.0/s
Equivalent rigid body observer gain	3958/s	2827/s
Vibration Suppression loop lowpass filter cutoff frequency	630 Hz	450 Hz
Vibration Suppression loop highpass filter cutoff frequency	15.5 Hz	15.4 Hz
Vibration Suppression loop gain	3.0	-2.0

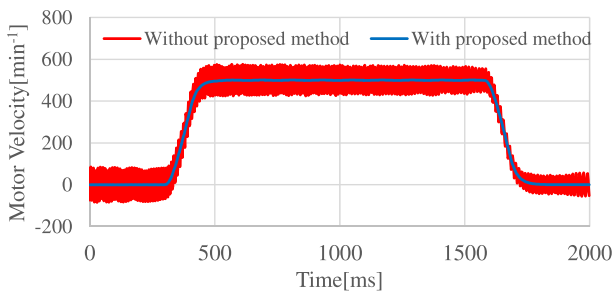


Fig. 9. Vibration suppression result of semi-closed system

controlled only with the motor encoder.

We observed the vibration waveform by increasing the velocity loop gain until vibration occurs. And we applied the proposed method and confirmed whether vibration was reduced. Table 1 shows the parameters during the experiment. Figure 9 shows the experimental results of the vibration suppression effect of the semi-closed system. When vibration suppression control is not applied, the vibration oscillates at 673 Hz, whereas applying the proposed method suppresses

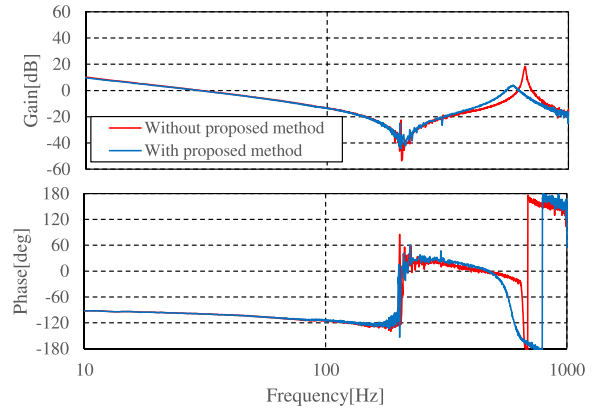


Fig. 10. Loop transfer characteristic of semi-closed system

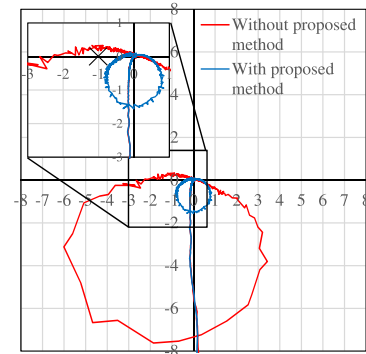


Fig. 11. Loop transfer characteristic of semi-closed system

the vibration.

In order to confirm the stability of the velocity loop, the Nyquist diagram is shown in Fig. 11, before and after applying the proposed method. Figure 11 was measured using a commercially available FFT analyzer. Before applying the proposed method, instability of the controller is shown, whereas stability is clearly improved after the application. At this time, the open loop frequency characteristics of the velocity changed before and after the applying the proposed method as shown in Fig. 10, and the Q factor of the resonance decreased from 52.8 to 9.0. In other words, by converting this to damping coefficient, it increased from 0.0095 to 0.0556.

5.2 Vibration Suppression Effect of Full-closed System

In the full-closed systems, velocity feedback is performed using the external encoder. We observed the vibration waveform by increasing the velocity loop gain until vibration occurs, similar to the semi-closed system. Next, we applied the proposed method and confirmed whether vibration was reduced. Table 1 shows the parameters during the experiment. Figure 12 shows the experiment result of the vibration suppression effect of the full-closed system. When vibration suppression control is not applied, the vibration oscillates at 581 Hz, whereas applying the proposed method suppresses the vibration.

In order to confirm the stability of the velocity loop, the Nyquist diagram in Fig. 14 shows the loop transfer characteristic before and after applying the proposed method. Figure 14 was measured using a commercially available FFT analyzer. Before applying the proposed method, instability of

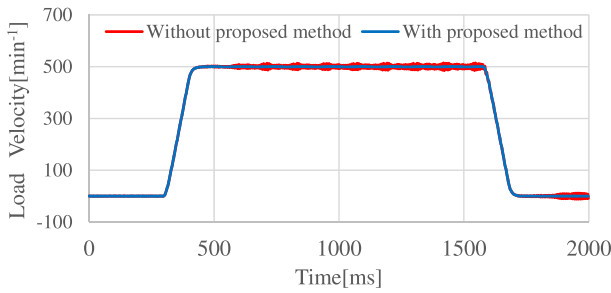


Fig. 12. Vibration suppression result of full-closed system

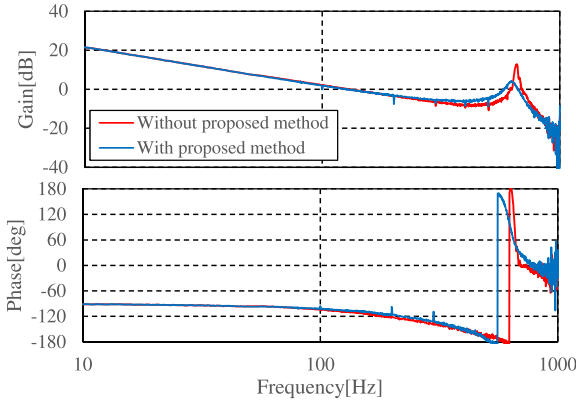


Fig. 13. Full-closed system loop transfer characteristic

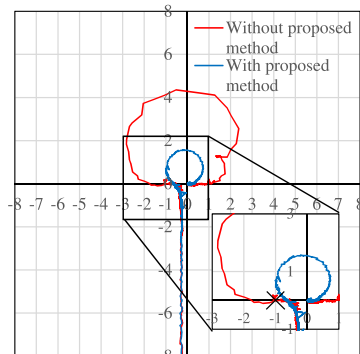


Fig. 14. Full-closed system loop transfer characteristic

the controller is shown, whereas stability is clearly improved after the application. At this time, the frequency characteristics of the velocity open loop changed before and after the application of the proposed method as shown in Fig. 13, and the Q factor of the resonance decreased from 32.9 to 11.4. In other words, by converting this to damping coefficient, it increased from 0.0152 to 0.0439.

6. Conclusion

In this paper, it is theoretically clarified that mechanical resonance characteristics can be damped in both semi-closed system and full-closed system by vibration suppression control based on the concept of “equivalent rigid body”. We also confirmed that the effects can be obtained by switching semi/full-closed control with the same experimental equipment. Also, in the proposed method, only the total moment of inertia of the controlled object and the gain K_d are necessary for the vibration control. This can greatly reduce the steps to identify the parameter of the controlled object, compared

to the damping control by an observer which has a nominal model of a general mechanical resonance system.

References

- (1) J. Oaki and S. Adachi: “Decoupling Identification and Physical Parameter Estimation for Serial Two-Link Two-Inertia System”, *IEE Japan*, Vol.128-D, No.5, pp.669–677 (2008) (in Japanese)
- (2) J. Oaki and S. Adachi: “Grey-box Modeling of Elastic-joint Robot with Harmonic Drive and Timing Belt”, *Proc. 16th IFAC Symposium on System Identification (SYSID2012)*, Brussels, pp.1401–1406 (2012)
- (3) M. Iwata, S. Itoh, and T. Ohno: “Identified System Parameter-Based Adaptive Vibration Control of a 2-Mass Resonant System”, *IEE Japan*, Vol.115-D, No.10, pp.1229–1236 (1995) (in Japanese)
- (4) Y. Tadano, T. Akiyama, M. Nomura, and M. Ishida: “Torque Ripple Suppression Control Based on the Periodic Disturbance Observer with a Complex Vector Representation for Permanent Magnet Synchronous Motors”, *IEE Japan*, Vol.132-D, No.1, pp.84–93 (2012) (in Japanese)
- (5) Y. Urakawa: “Experiment of High Gain Servo System for Optical Disk Drives”, *Proc. 47th Proceedings of the Japan Joint Automatic Control Conference*, Session ID801 (2005) (in Japanese)
- (6) Y. Urakawa: “Parameter Design for a Digital Control System with Calculation Delay Using a Limited Pole Placement Method”, *IEE Japan*, Vol.133-D, No.3, pp.272–281 (2013) (in Japanese)
- (7) S. Kawahara, T. Yoshioka, K. Ohishi, N. Hien, T. Miyazaki, and Y. Yokokura: “Vibration Suppression Control Method using Extended State Observer for Angular Transmission Error in Cycloid Gear”, *IEE Japan*, Vol.134-D, No.3, pp.241–251 (2014) (in Japanese)
- (8) K. Oishi, T. Myoui, K. Ohnishi, and K. Miyachi: “One Approach to Speed Control of dc Motor Having two Inertia Resonant System”, *IEE Japan*, Vol.106-B, No.2, pp.31–38 (1986) (in Japanese)
- (9) K. Koyama: “Design of Speed Control Systems of Motor with Elastically Coupled Load making use of Reference Model”, *Proc. National Convention record IEE Japan, Industry Applications Society*, pp.451–456 (1987) (in Japanese)
- (10) Y. Hori: “Comparison of Vibration Suppression Control Strategies in 2-Mass Systems including a Novel Two-Degrees-Of-Freedom H_∞ Controller”, *Proc. IEEE AMC'92*, pp.409–416 (1992)
- (11) T. Hasegawa, R. Kurosawa, H. Hosoda, and K. Abe: “A Microcomputer-Based Motor Drive System with Simulator Following Control”, *IEEE-IECON*, p.41 (1986)
- (12) Y.F. Chen, K. Fujikawa, and H. Kobayashi: “Observer Based Torsional Torque Control of Vibration Systems”, *1993 IEE Japan Industry Applications Society Conference* (in Japanese)

Yasufumi Yoshiura (Member) received the B.Sc. and M.Sc. degrees from Kyushu University, Fukuoka, Japan, in 2000. The same year, he joined YASKAWA ELECTRIC CORPORATION, Japan. He has been engaged in developing technology of mechatronics-system.



Shouta Kawahara (Member) received B.Sc. and M.Sc. degrees from Nagaoka University of Technology, Niigata, Japan in 2011 and 2013. In 2013, he joined YASKAWA ELECTRIC CORPORATION, Japan. He has been engaged in developing technology of motion control.



Daichi Horimai



(Non-member) received the B.Sc. and M.Sc. degree from S.U.N.Y Stony Brook University, New York, United States, in 2011. The same year, he joined YASKAWA ELECTRIC CORPORATION, Japan. He had been working as an embedded mechatronics-system software development, and currently working as a business planning team.

Yasuhiko Kaku



(Senior Member) received the M.Sc. degree from Kyushu Institute of Technology, Fukuoka, Japan, in 1982. The same year, he joined YASKAWA ELECTRIC CORPORATION, Japan. And he received the Ph.D. from Chiba University, Chiba, Japan, in 1988. He has been engaged in developing technology of mechatronics-system.

Tetsuya Asai



(Member) received B.Sc., M.Sc. degrees in electrical engineering from the Nagaoka University of Technology, Niigata, Japan, in 2008 and 2010, respectively. In 2010, he joined YASKAWA ELECTRIC CORPORATION, Iruma, Japan. He has worked on development of motor-drive control. He is a member of Institute of Electrical Engineers of Japan.